Analysis of coastline extraction indices using Sentinel-2 and Google Earth Engine, case study in Bali, Indonesia

Amandangi Wahyuning Hastuti[1,2], *Neira Purwanty* Ismail[3,*], and *Masahiko* Nagai[1]

[1]Graduate School of Science and Technology for Innovation, Yamaguchi University, 2-16-1 Tokiwadai, Ube, Yamaguchi Prefecture 755-8611, Japan
[2]Institute for Information Management of Marine and Fisheries Resources, Ministry of Marine Affairs and Fisheries of the Republic of Indonesia, Bali, 82251, Jembrana, Indonesia
[3]Department of Fisheries Technology Engineering, Faculty of Marine Sciences, Karadeniz Technical University, Trabzon 61530, Turkiye

Abstract. Coastal zone is the most dynamic environment and requires regular monitoring to maintain sustainable coastal resource management. Employing remote sensing technology to monitor changes involves an essential process referred to as coastline extraction. This study aims to conduct a comparative analysis of five commonly employed techniques for coastline extraction: Normalized Difference Vegetation Index (NDVI), Normalized Difference Water Index (NDWI), Modified Normalized Difference Water Index (MNDWI), Water Ratio Index (WRI), and Automated Water Extraction Index (AWEI). These methods are evaluated by automatically delineating sandy beaches and coastlines using high-resolution imagery from the Sentinel-2 satellite for Bali, Indonesia. The Otsu algorithm is utilized to determine the optimal threshold value. Compared to the other indices, the results indicate that MNDWI proved to be the most effective in highlighting water bodies, with the average distance from the validated point of MNDWI being 12.9 m and a Mean Absolute Error (MAE) of 7.11, whereas NDVI demonstrated a high level of proficiency in detecting coastal vegetation. This study highlights the potential of utilizing both Sentinel-2 satellite imagery and the Google Earth Engine (GEE) platform for efficient coastline monitoring. This study also provides scientific evidence supporting the reliability and accuracy of coastline extraction through spectral water indices.

1 Introduction

Coastal regions offer abundant, invaluable natural resources and serve as a vital source of sustenance for human populations [1]. These areas have experienced various human activities and interventions [2]. Their appeal stems from their typically level terrain and pivotal positioning at the intersection of land and sea, making them preferred locations for development [3,4]. Many of the world's most populated and well-known cities are near or on

* Corresponding author: neira.ismail@gmail.com

the continent's coastlines [5]. Over half the global population lives in coastal regions, comprising only 10% of the Earth's surface [6]. Nevertheless, the effective management of coastal zones is often hindered by land use conflicts arising from the competing demands and pressures associated with human activities [7].

The coastline, a dynamic part of coastal regions, undergoes continuous transformation [8,9]. Alterations in the coastline characterized by its movements towards the sea are called sedimentation, while shifts towards the land are known as erosion or abrasion [10,11]. Natural processes such as wind, waves, and currents, as well as extreme climatic conditions, can instigate either erosion or sedimentation on the coastline, but external factors, primarily human activities, can potentially accelerate or impact the rate of coastline change [12,13]. Human interventions can potentially disrupt the fragile equilibrium of sediment movement along the coast, ultimately contributing to the degradation of coastal areas and ecosystem services [14,15].

Monitoring and documenting a specific region over a defined timeframe are crucial for assessing changes along the coastline [16]. Access to coastline alteration trends and rate data is fundamental for effective coastal zone management planning [17]. Remote sensing technology is generally cost-effective for acquiring spatial data, enabling the detection of Earth's features without direct physical contact [18,19]. Additionally, it offers access to historical image archives captured at different times (multi-temporal) [20]. The widespread use of near-infrared bands (NIR) has proven valuable in distinguishing between water bodies and land, particularly for coastline delineation [21]. Moreover, DeWitt [22] has emphasized that the water's absorption of infrared wavelengths and the strong reflectance of vegetation and soil in these images make them ideal for mapping the spatial distribution of land and waterbody.

The coastal zone requires regular and precise monitoring as an essential component in maintaining sustainable coastal resource management since it is one of the planet's most dynamic and constantly changing environments [23]. In order to accurately assess and comprehend the fluctuations and transformations within this highly dynamic coastal region, this critical monitoring effort depends on using advanced remote sensing technologies [24]. The complex procedure known as coastline extraction, which allows the accurate identification and characterization of coastal features and their changes over time, is an essential aspect of this technical approach [25,26]. Furthermore, it is necessary to adjust the coastline for the tidal effect as a reference to present accurate and unbiased coastline data [27].

The Bali Islands are well-known in Indonesia as a popular tourist destination [28,29]. The local population relies heavily on marine and coastal resources for their livelihood. Alongside tourism and agriculture, services and trade are essential economic drivers on the island [29,30]. Bali's coastal areas significantly contribute to the island's social and economic development. Nevertheless, an investigation by Hastuti et al. [31] revealed that nearly half of the island's coastline is highly vulnerable. Karang Dadi Beach and the southern coast of Bali are among the most vulnerable beaches due to the area's rapid erosion (not yet published).

This study compares five well-known methods widely employed for the automatic extraction of coastlines. These methods include the Normalized Difference Vegetation Index (NDVI), Normalized Difference Water Index (NDWI), Modified Normalized Difference Water Index (MNDWI), Water Ratio Index (WRI), and Automated Water Extraction Index (AWEI). The study assesses the effectiveness of these approaches, specifically in the context of automatically outlining the complex sandy beach coastline. In order to do this, the study employed high-resolution imagery obtained from the Sentinel-2 satellite, focusing on the sandy coastal area of Bali, Indonesia, as the study area. In order to improve the accuracy and precision of the coastline extraction process, the Otsu algorithm is also employed as a critical tool for choosing the best threshold value for image processing.

2 Methodology

2.1 Characteristics of the study area

This study was conducted at Karang Dadi Beach, situated in the Klungkung Regency of Bali Province, Indonesia. The study area has sandy beaches and a 3.5 km coastline. Karang Dadi Beach is approximately 35.5 km from Denpasar, the provincial capital of Bali, Indonesia.

Bali Province is central to the Indonesian archipelago and is renowned as a prime tropical destination for domestic and international tourists [28,29]. As of the 2020 census, the population of Bali Province was estimated to be around 4.317.404 [32]. The majority of this population heavily relies on coastal and marine resources for their livelihoods, and consequently, many essential public facilities and services have been established in coastal areas [33]. However, this region has faced challenges such as rapid coastal erosion and land subsidence, primarily attributed to the excessive exploitation of coastal resources [34,35]. Given the characteristics of the beaches and the challenges presented by the area's rapid coastal erosion, this area was selected as a study area. The location of the study area is shown in Figure 1.

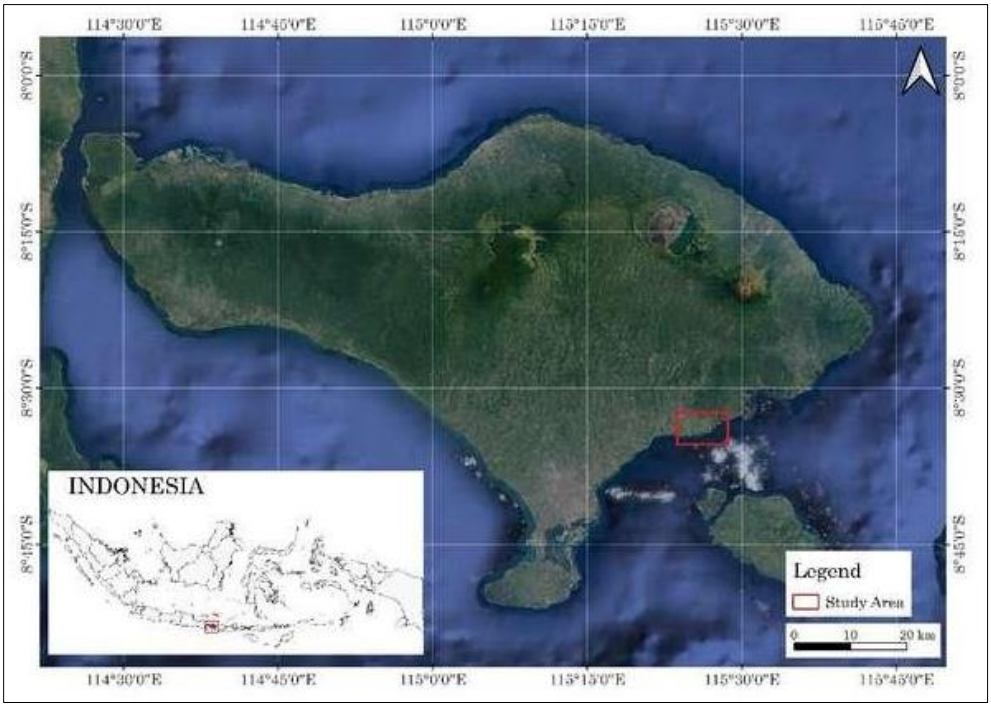

Fig. 1. The study area is located in the southeast of Bali Island, Indonesia.

2.2 Datasets

To determine the coastline position, the present study employed a Sentinel-2 image with acquisition data on March 13, 2023. The image was subjected to orthorectification using the WGS84 datum and UTM Zone 51 south projection. A field survey on March 13, 2023, was also undertaken along the study area to validate the study. In addition, PlanetScope ortho-tile imagery with acquisition data on June 13, 2021, was used as the base map and comparison.

Sentinel-2, a high-resolution satellite system operated by the European Space Agency (ESA), was launched on June 23, 2015, and is available for public use at no cost [36]. Its primary mission is to monitor various aspects of the Earth's surface, including land, vegetation, water bodies, and coastal regions [37]. The satellite has 13 distinct spectral bands, each serving a specific purpose (**Table 1**). In applications related to coastline detection, the spectral bands of particular relevance are the visible bands (Blue, Green, and Red), the near-infrared band (NIR), and the short-wave infrared band (SWIR) [38–40].

Table 1. Sentinel-2 Multi-Spectral Instrument (MSI) sensor.

Bands	Central wavelength (nm)	Resolution (m)	Band Description
B1	443	60	Ultra-Blue (Coastal and Aerosol)
B2	490	10	Blue
B3	560	10	Green
B4	665	10	Red
B5	705	20	Visible and Near Infrared (VNIR)
B6	740	20	Visible and Near Infrared (VNIR)
B7	783	20	Visible and Near Infrared (VNIR)
B8	842	10	Visible and Near Infrared (VNIR)
B8a	865	20	Visible and Near Infrared (VNIR)
B9	940	60	Short Wave Infrared (SWIR)
B10	1375	60	Short Wave Infrared (SWIR)
B11	1610	20	Short Wave Infrared (SWIR)
B12	2190	20	Short Wave Infrared (SWIR)

PlanetScope is a high-resolution imaging satellite constellation launched in 2016. It captures detailed images of land, vegetation, water, and coasts, providing data similar to the European Space Agency's Sentinel-2 mission. PlanetScope images have a resolution of 3 meters per pixel and include eight spectral bands for capturing a wider range of information, as shown in **Tabel 2**.

Table 2. PlanetScope Multi-Spectral Instrument (MSI) sensor [41].

Bands	Central wavelength (nm)	Resolution (m)	Band Description
B1	443	3	Coastal Blue
B2	490		Blue
B3	531		Green I
B4	565		Green
B5	610		Yellow
B6	665		Red
B7	705		Red Edge
B8	865		NIR

2.3 Coastline extraction

In this study, five indices were used to delineate the sandy coast in the study area: the Normalized Difference Vegetation Index (NDVI), the Normalized Difference Water Index (NDWI), the Modified Normalized Difference Water Index (MNDWI), the Water Ratio Index (WRI), and the Automated Water Extraction Index (AWEI) [42].

The Normalized Difference Vegetation Index (NDVI) assesses vegetation density and health status. It also applies to coastal vegetation and coastline delineation [43–45]. The NDVI is defined by Equation 1.

$$NDVI = \frac{NIR - Red}{NIR + Red} \quad (1)$$

The Normalized Difference Water Index (NDWI) method was developed by McFeeters [46] and is widely employed for water body extraction. This method employs green and near-infrared bands to differentiate between water and non-water pixels [47,48]. As a result, water features yield positive values, while vegetation and soil features produce zero or negative values—the NDWI defined by Equation 2.

$$NDWI = \frac{Green - NIR}{Green + NIR} \quad (2)$$

The Modified Normalized Difference Water Index (MNDWI) is a variation of the NDWI method initially formulated by Xu [49]. Using green and short-wave infrared bands, MNDWI effectively distinguishes between water bodies and land features. This process yields a grayscale image with values from -1 to 1 [47,48]. The MNDWI is defined by Equation 3.

$$MNDWI = \frac{Green - SWIR}{Green + SWIR} \quad (3)$$

The Water Ratio Index (WRI) is derived from water's primary spectral reflection characteristics in the green and red bands, incorporating data from four spectral reflectance bands [47]. The WRI is defined by Equation 4.

$$WRI = \frac{Green + NIR}{NIR + SWIR} \quad (4)$$

The Automated Water Extraction Index (AWEI) enhances the identification of coastlines by heightening the distinction between water and other surfaces, thus optimizing the differentiation between water and non-water pixels [47,48]. The AWEI is defined by Equation 5.

$$AWEI = BLUE + 2.5 * GREEN - 1.5 * (NIR + SWIR1) - 0.25 * SWIR2 \quad (5)$$

The process of coastline extraction can be divided into two main phases: image pre-processing and image analysis. Both phases were executed using the Google Earth Engine (GEE) platform, while image visualization was carried out with an open-source GIS program such as QGIS 3.28 LTR [50]. Figure 2 visualizes the present study's workflow.

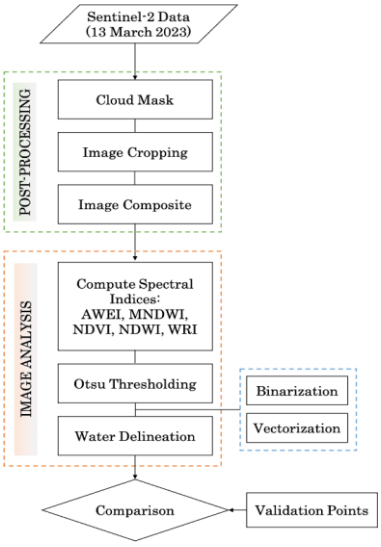

Fig. 2. Flowchart of coastline extraction indices comparison.

The otsu's method involves finding an optimal threshold based on the observed distribution of pixel values [51,52] and an acceptable method for achieving stable temporality classification for time series analysis. Otsu's segmentation method can effectively separate land from water along the coast [51,53,54].

3 Results and Discussion

In the present study, a 3.5 km long coastline was automatically delineated and mapped on Sentinel-2 images by performing five widely employed indices for coastline extraction (NDVI, NDWI, MNDWI, WRI, and AWEI). Karang Dadi Beach is characterized by sandy beaches with varying widths or distances to various land cover/land use, and coastal vegetation. These varying beach characteristics generally distinguish the performance results of the applied coastline extraction indices.

In the present study, high-resolution satellite images from PlanetScope were employed for coastline mapping, and the resulting coastlines were utilized as the baseline (reference) for calculating coastline length. The coastline length determined through on-screen digitization was measured at 2.985 m, covering an area of 652.867 km2.

3.1 Normalized Difference Vegetation Index (NDVI)

The study obtained a shoreline of 4.983 m with a difference of 1.998 m from the reference coastline by using the NDVI index to detect coastlines in the study area. The results revealed that NDVI performed exceptionally better in identifying coastal vegetation. Based on visual interpretation, the index provides a precise coastline where the coast is adjacent to vegetated coasts. According to Esendağlı et al. [55] and Selim et al. [42], the NDVI can identify objects according to their moisture content and has demonstrated its superior performance in vegetated coastal areas. As a result, NDVI had limitations in detecting dunes and rocky shores within the study area. The result of NDVI is shown in Figure 3.

Fig. 3. Result of coastline extraction using the Normalized Difference Vegetation Index (NDVI).

3.2 Normalized Difference Water Index (NDWI)

The study obtained a coastline of 4.409 m with a difference of 1.424 m from the reference coastline by using the NDWI index to detect coastlines in the study area. According to data based on visual interpretation, NDWI outperformed NDVI in identifying coastlines. Due to its coverage of the study area's rocky coasts and dunes, the index produces higher results for sandy beaches. According to a study by Wicaksono and Wicaksono [48], the NDWI also performed best in identifying artificial coasts. The result of NDWI is shown in Figure 4.

Fig. 4. Result of coastline extraction using the Normalized Difference Water Index (NDWI).

3.3 Modified Normalized Difference Water Index (MNDWI)

The coastline length obtained in this study, which used the MNDWI index to detect coastlines in the study region, was 4.169 m, a difference from the reference coastline of 1.184 m. The results of the visual interpretation showed that MNDWI outperformed NDWI and NDVI in locating the shoreline. NDWI and MNDWI results were found to be closely related. The MNDWI index is sensitive to sediment shadow, which is advantageous for shoreline extraction, according to Li et al. [56]. With an accuracy rate of 99.85 percent, MNDWI was often used to map water bodies and was thought to be the most incredible tool to differentiate between water and land features [49]. The result of MNDWI is shown in Figure 5.

Fig. 5. Result of coastline extraction using the Modified Normalized Difference Water Index (MNDWI).

3.4 Water Ratio Index (WRI)

The WRI index was used in this study's shoreline detection in the study area, where the coastline measured 6.649 meters, which was longer than the reference coastline of 3.664 meters. Based on visual interpretation, the findings showed that WRI performed poorly in the research area when recognizing shorelines compared to NDWI and NDVI. The result of WRI is shown in Figure 6.

Fig. 6. Result of coastline extraction using the Water Ratio Index (WRI).

3.5 Automated Water Extraction Index (AWEI)

This study used the AWEI index for shoreline detection in the study area with a coastline length of 4.210 m, resulting in a deviation from the reference coastline of 1.225 m. Based on visual interpretation, AWEI performed better than the WRI index and was close to the MNDWI results. This result demonstrated continuity along the study area's coast. According to a study conducted by Selim et al. [42], the unique property of absorbing more MIR light (SWIR-2) than NIR light gives AWEI positive results. The result of AWEI is shown in Figure 7.

Fig. 7. Result of coastline extraction using the Automated Water Extraction Index (AWEI).

Figure 8 shows the comparison results of all employed indices. **Table 3** compares the five applied coastline extraction indices to the validated points.

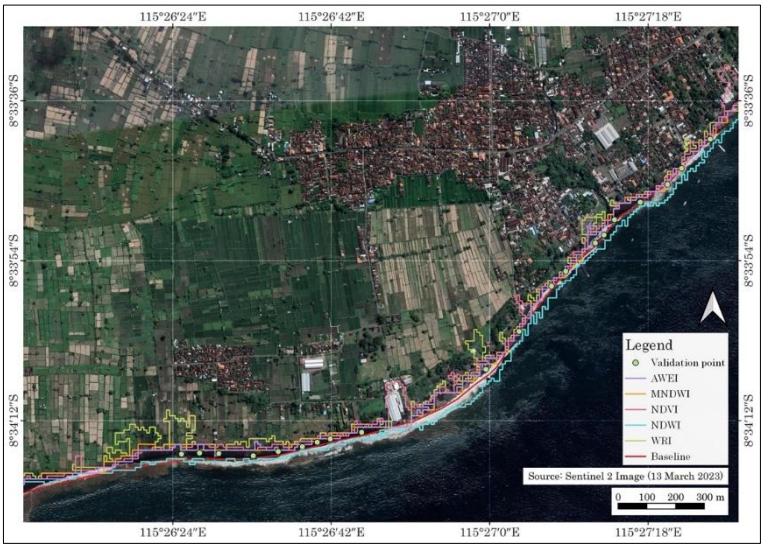

Fig. 8. Comparison results of coastline extraction using all the indices.

Table 3 shows that MNDWI, followed by AWEI, NDWI, and NDVI indices, performed close to the validated points and had the lowest Mean Absolute Error (MAE) with 7.11. The MAE measures the average of the residuals in the dataset. Meanwhile, WRI was the result that performed the furthest from the reference. Furthermore, manual on-screen digitization techniques are time-consuming and labor-intensive, yet they produce high-quality results. The application of these indices made it possible to detect coastlines faster than using Sentiel-2 satellite imagery. Several studies have proven that MNDWI provides higher accuracy than NDWI and other coastline extraction indices [48].

Table 3. Comparison of all applied indices to the validated points.

Index	Length (m)	Area (m2)	Difference		The average distance from the validated point	The Mean Absolute Error (MAE)
			Length (m)	Area (m2)		
NDVI	4.983	698.905	-1.998	-46.038	21.270	8.78
NDWI	4.409	687.548	-1.424	-34.681	28.517	9.04
MNDWI	4.169	646.383	-1.184	6.484	12.901	7.11
WRI	6.649	574.953	-3.664	77.914	35.200	19.65
AWEI	4.210	635.283	-1.225	17.584	15.763	9.59
Baseline	***2.985***	***652.867***				

The results of our study highlight the effectiveness of the Modified Normalized Difference Water Index (MNDWI) in accentuating water bodies, demonstrating its superior performance in this crucial aspect of coastline analysis. The Normalized Difference Vegetation Index (NDVI) similarly shows an exceptional capacity for identifying and characterizing coastal vegetation, reflecting a high level of proficiency in this regard. A thoughtfully chosen threshold is essential for precise application. These results contribute to advancing our understanding of coastline extraction techniques and highlight the great potential to enhance the effectiveness of coastline monitoring by combining Sentinel-2 satellite images with the robust Google Earth Engine (GEE) platform.

The use of spectral water indicators in this work also provides solid scientific support for the accuracy and dependability of shoreline extraction. As a result, remote sensing is proven to be a valuable technique for managing coastal resources, and its crucial role in guaranteeing the sustainability of coastal ecosystems and resources in places like Bali, Indonesia, and elsewhere is highlighted. The implications of these findings extend beyond the confines of this study, providing insightful information and prospects for improvements in coastal monitoring and environmental conservation initiatives.

4 Conclusion

This study underscores the significance of employing advanced remote sensing technology for continuously monitoring and managing coastal zones, which are inherently dynamic environments. The comparative analysis of five prominent coastline extraction techniques revealed that the Modified Normalized Difference Water Index (MNDWI) is the most effective method for delineating water bodies along sandy beaches. In contrast, the Normalized Difference Vegetation Index (NDVI) displayed a commendable ability to detect coastal vegetation. These findings demonstrate the potential of harnessing high-resolution imagery from the Sentinel-2 satellite and leveraging the Google Earth Engine (GEE) platform for efficient and accurate coastal monitoring. Additionally, stakeholders and policymakers should consider investing in continued remote sensing-based monitoring efforts to ensure the sustainability of coastal ecosystems and resources in regions such as Bali, Indonesia. Further

research could explore the applicability of these techniques in other coastal areas to broaden their practical utility in coastal resource management worldwide.

This study was funded by the Japan International Cooperation Agency (JICA) and supported by Yamaguchi University. We thank the European Space Agency for providing the Sentinel-2 imagery data and the Google Earth Engine developer for providing an open-source GIS platform.

References

1. B. Neumann, K. Ott, and R. Kenchington, Sustain Sci **12**, 1019 (2017)
2. W. Chen, D. Wang, Y. Huang, L. Chen, L. Zhang, X. Wei, M. Sang, F. Wang, J. Liu, and B. Hu, Sci Rep **7**, 1 (2017)
3. I. P. Citra and A. S. Nugraha, (2021)
4. W. Cao and M. H. Wong, Environ Int **33**, 985 (2007)
5. UNR Seas, *Percentage of Total Population Living in Coastal Areas* (2007)
6. B. Neumann, A. T. Vafeidis, J. Zimmermann, and R. J. Nicholls, PLoS One **10**, (2015)
7. R. Susman, A. M. Gütte, and T. Weith, Land 2021, Vol. 10, Page 615 **10**, 615 (2021)
8. K. Uddin, N. Khanal, S. Chaudhary, S. Maharjan, and R. B. Thapa, Environmental Challenges **1**, 100001 (2020)
9. L. Zhang, H. Shi, H. Xing, P. Li, and P. Ma, Front Mar Sci **10**, 1232060 (2023)
10. L. Mentaschi, M. I. Vousdoukas, J. F. Pekel, E. Voukouvalas, and L. Feyen, Scientific Reports 2018 8:1 **8**, 1 (2018)
11. A. C. Narayana, Encyclopedia of Earth Sciences Series 590 (2016)
12. T. Islam and J. Ryan, Hazard Mitigation in Emergency Management 275 (2016)
13. S. Kurt, A. Karaburun, and A. Demirci, Scientific Research and Essays **5**, 3009 (2010)
14. F. Ahmet Sesli, International Journal of the Physical Sciences **5**, 1567 (2010)
15. Y. Ge and J.-Y. Zhang, (2011)
16. S. Dellepiane, R. De Laurentiis, and F. Giordano, (2004)
17. R. S. Dewi and W. Bijker, The Egyptian Journal of Remote Sensing and Space Science **23**, 181 (2020)
18. E. F. Lambin, International Encyclopedia of the Social & Behavioral Sciences 13150 (2001)
19. B. Janga, G. P. Asamani, Z. Sun, and N. Cristea, Remote Sensing 2023, Vol. 15, Page 4112 **15**, 4112 (2023)
20. C. Chen, J. Liang, F. Xie, Z. Hu, W. Sun, G. Yang, J. Yu, L. Chen, L. Wang, L. Wang, H. Chen, X. He, and Z. Zhang, International Journal of Applied Earth Observation and Geoinformation **107**, 102711 (2022)
21. J. P. Mondejar and A. F. Tongco, Sustainable Environment Research **1**, 1 (2019)
22. A. A. Alesheikh, A. Ghorbanali, and N. Nouri, International Journal of Environmental Science & Technology 2007 4:1 **4**, 61 (2007)
23. A. Melet, P. Teatini, G. Le Cozannet, C. Jamet, A. Conversi, J. Benveniste, and R. Almar, Surveys in Geophysics 2020 41:6 **41**, 1489 (2020)

24. Q. Zhao, J. Pan, A. T. Devlin, M. Tang, C. Yao, V. Zamparelli, F. Falabella, and A. Pepe, Remote Sensing 2022, Vol. 14, Page 2384 **14**, 2384 (2022)
25. X. Zhou, J. Wang, F. Zheng, H. Wang, and H. Yang, Remote Sensing 2023, Vol. 15, Page 4865 **15**, 4865 (2023)
26. F. Domazetović, A. Šiljeg, I. Marić, J. Faričić, E. Vassilakis, and L. Panđa, Applied Sciences (Switzerland) **11**, 9482 (2021)
27. K. Vos, K. D. Splinter, J. Palomar-Vázquez, J. E. Pardo-Pascual, J. Almonacid-Caballer, C. Cabezas-Rabadán, E. C. Kras, A. P. Luijendijk, F. Calkoen, L. P. Almeida, D. Pais, A. H. F. Klein, Y. Mao, D. Harris, B. Castelle, D. Buscombe, and S. Vitousek, Communications Earth & Environment 2023 4:1 **4**, 1 (2023)
28. G. K. Sutawa, in *Procedia Economics and Finance* (Elsevier, 2012), pp. 413–422
29. M. Antara and M. S. Sumarniasih, Journal of Tourism and Hospitality Management **5**, 34 (2017)
30. A. Rajendra, in *IOP Conf. Series: Earth and Environmental Science 423* (IOP Publishing, 2019)
31. A. W. Hastuti, M. Nagai, and K. I. Suniada, Remote Sensing 2022, Vol. 14, Page 4409 **14**, 4409 (2022)
32. R. N. T. Amboro, N. Saptari, and N. P. P. Syanthi, *Provinsi Bali Dalam Angka 2022 - Bali Province in Figures 2022* (Badan Pusat Statistik (BPS) Provinsi Bali, 2022)
33. A. Furqan and F. I. Winandi, ASEAN Journal on Hospitality and Tourism **16**, 84 (2018)
34. A. Rajendra, in *the 4th International Conference on Climate Change 2019, IOP Conf. Series: Earth and Environmental Science 423* (IOP Publishing, 2020)
35. Mujiburrahman, Y. Rochwulaningsih, S. T. Sulistiyono, and M. P. Utama, in *E3S Web of Conferences 202 ICENIS 2020* (2020), p. 10
36. Copernicus Sentinel-2 (processed by ESA), *MSI Level-1C TOA Reflectance Product. Collection 1* (2021)
37. K. Kaku, International Journal of Disaster Risk Reduction **33**, 417 (2019)
38. F. Uhl, T. G. Rasmussen, and N. Oppelt, Geosciences (Switzerland) **12**, 15 (2022)
39. A. S. Mansaray, A. R. Dzialowski, M. E. Martin, K. L. Wagner, H. Gholizadeh, and S. H. Stoodley, (2021)
40. K. Darwish and S. Smith, Engineering Proceedings 2021, Vol. 10, Page 23 **10**, 23 (2021)
41. Planet, *Planet Imagery Product Specifications* (Planet Labs Inc., 2018)
42. S. Selim, Ç. Esendağlı, and B. Dönmez, in *Recent Studies in Planning and Design*, edited by A. Altuntaş and Ş. Alp (IKSAD Publishing House, Ankara, 2022), pp. 3–24
43. S. Guha, International Journal of Advanced Biological Research **6**, 253 (2016)
44. T. V. Tran, R. Reef, and X. Zhu, Remote Sensing 2022, Vol. 14, Page 4868 **14**, 4868 (2022)
45. M. R. Akbar, P. A. A. Arisanto, B. A. Sukirno, P. H. Merdeka, M. M. Priadhi, and S. Zallesa, IOP Conf Ser Earth Environ Sci **584**, 012069 (2020)
46. S. K. McFeeters, Int J Remote Sens **17**, 1425 (1996)
47. J. Laonamsai, P. Julphunthong, T. Saprathet, B. Kimmany, T. Ganchanasuragit, P. Chomcheawchan, and N. Tomun, Hydrology 2023, Vol. 10, Page 70 **10**, 70 (2023)

48. A. Wicaksono and P. Wicaksono, Geoplanning: Journal of Geomatics and Planning **6**, 55 (2019)
49. H. Xu, Int J Remote Sens **27**, 3025 (2007)
50. QGIS Development Team, (2022)
51. W. Tang, C. Zhao, J. Lin, C. Jiao, G. Zheng, J. Zhu, X. Pan, and X. Han, Water 2022, Vol. 14, Page 855 **14**, 855 (2022)
52. N. Otsu, IEEE Trans Syst Man Cybern **SMC-9**, 62 (1979)
53. K. Vos, K. D. Splinter, M. D. Harley, J. A. Simmons, and I. L. Turner, Environmental Modelling & Software **122**, 104528 (2019)
54. S. P. Viaña-Borja and M. Ortega-Sánchez, Remote Sensing 2019, Vol. 11, Page 2186 **11**, 2186 (2019)
55. Ç. Esendağlı, S. Selim, and N. Demir, in *4th Intercontinental Geoinformation Days* (Tabriz, Iran, 2022), pp. 199–202
56. Z. Li, H. Chen, and Q. Nie, (2021)